Preprint Title	A Novel Dry Blending Method to Reduce Coefficient of Thermal Expansion of Polymer Template for OTFT Electrodes Alignment
Authors	Xiangdong Ye, Bo Tian and Yuxuan Guo
Publication Date	12 Dez 2019
Article Type	Full Research Paper
ORCID® iDs	Xiangdong Ye - https://orcid.org/0000-0001-7534-2986

A Novel Dry Blending Method to Reduce Coefficient of Thermal Expansion of Polymer Template for OTFT Electrodes Alignment

Xiangdong Ye*, Bo Tian, Yuxuan Guo

School of Mechanical and Electrical Engineering
Shaanxi Key Laboratory of Nano Materials and Technology
Xi'an University of Architecture and Technology
Xi'an 710055, China
Tel: 86-029-82202553
Fax: 86-029-82202552
* E-mail: yexiangd@xauat.edu.cn

Abstract: Among patterning technologies for organic thin-film transistors (OTFT), the fabrication of OTFT electrodes using polymer template has attracted much attention. However, deviations in electrodes alignment occur owing to a much higher coefficient of thermal expansion (CTE) of the polymer template than the CTE of the dielectric layer. Here, a novel dry blending method is described in which SiO_2 nanoparticles are filled into a grooved silicon template, following by permeation of polydimethylsiloxane (PDMS) into the SiO_2 nanoparticle gaps. The SiO_2 nanoparticles in the groove are extracted by curing and peeling off PDMS to prepare a PDMS/SiO_2 composite template with a nanoparticle content of 83.8 wt%. The composite template has a CTE of 96 ppm/°C, which a reduction of 69.23%, compared with the original PDMS template. Finally, we achieved the OTFT electrodes alignment by the composite template.

Keywords: PDMS/SiO_2 composite template; dry blending; coefficient of thermal expansion; OTFT electrodes

1. Introduction

Organic thin-film transistors (OTFT) provide a platform to construct the next-generation large-area, light-weight, flexible, and stretchable optoelectronic applications [1,2], including flexible displays [3], electronic paper [4], sensors [5], and medical applications [6], etc. Fabricating high-performance OTFT usually requires that the electrodes on the polymer template can exhibit a precise alignment [7]. However, the polymer template has a high coefficient of thermal expansion (CTE), resulting in alignment deviations of the OTFT electrodes [8,9].

Currently, one of the measures to reduce the CTE of polymer template is wet blending, in which the low CTE nanomaterial is directly incorporated in a polymer to obtain a composite. Shokrieh et al. [10] through a systematic theoretical study to

investigate carbon nanotubes (CNTs) effects on CTE of CNT/epoxy, and the results indicate that addition of 1 wt% CNT causes the matrix CTE to decrease more significantly. González-Benito et al. [11] used a high energy ball cryomilling to uniformly disperse 5 wt% of titanium dioxide (TiO_2) nanoparticles (a size of 65 nm) within Poly(ethylene-co-vinyl acetate) (EVA) to subsequently obtain a film of the composite with lower CTE by hot pressing. Furthermore, Ren et al. [12] first prepared the sol-gel precursor by tetraethyl orthosilicate (TEOS) added to polyvinyl pyrrolidone (PVP), and then synthesized silica/PVP nanofiber composite by electrospinning process. The content of silica nanofiber in the composite is 9.1 wt%, and its CTE is decreased by ~40%. Jeyranpour et al. [13] studied the effects of fullerene (C_{60}) on the CTE of Araldite LY 5052/Aradur HY 5052 cross-linked resin epoxy by molecular dynamics simulation. The CTE was minimized by adding a maximum of 15.9 wt% fullerene to the LY/HY/C_{60} epoxy system. Liu et al. [14] selected MCM-41 mesoporous silica nanoparticles (a size of 300 nm) to be doped into polydimethylsiloxane (PDMS) to prepare a PDMS/MCM-41 nanocomposite. The CTE of the nanocomposite decreased from the original 301 (original PDMS) to 241 ppm/°C, when the content of silica in PDMS increased to 20 wt%. To further reduce the CTE of the polymer template, Kalsoom et al. [15] treated the non-porous HPHT microdiamond powder (a size of 2~4 μm) with sodium hydroxide and nitric acid followed by intensive washing with deionised water to reduce their tendency to agglomerate. The 30 wt% of the synthetic microparticles added to the acrylate polymer to reduce the CTE of the composite. More recently, Wang et al. [16] hydrolyzed various organic compounds to synthesize APrTEOS-capped poly (amic acid) solution (EPI) by the sol-gel method, and then added the maximum content of 32.16 wt% tetramethyl orthosilicate (TMOS) and water (as a diluent) into the EPI to prepare a polyimide-silica hybrid film having a low CTE.

However, because of the poor dispersion of the nanomaterial and the high viscosity of the polymer during the wet blending process [17,18], the nanomaterial content in the composite is usually low, which causes the CTE of the polymer template remain high [19]. Hence, we propose a novel dry blending method, in which nanomaterial is filled into the grooves of the patterned template firstly, and then the liquid polymer is poured on the template. As the polymer will permeate into the gaps of the nanomaterial to form the composite, the resultant composite can possess high content of the nanomaterial. In this paper, a PDMS/SiO_2 composite template with a SiO_2 nanoparticle content of 83.8 wt% is prepared by the dry blending. Compared to the original PDMS template having a CTE of 312 ppm/°C, the composite template

exhibits a CTE of 96 ppm/°C. Using the composite template with the low CTE, we achieved well alignment of the OTFT electrodes.

2. Experimental

2.1. Materials

SiO_2 nanoparticles of size 500 nm were provided by XFNANO Materials (Nanjing, China). PDMS (Sylgard 184), consisting of a base and curing agent, was purchased from Dow Corning Corporation. Silver target ofφ 60 × 5 mm in size and purity of 99.99% as the OTFT electrodes material was purchased from ZHNOGNUO New Material Co., Ltd., (Beijing, China). The pentacene as the semiconductor layer was used as purchased from Sigma Aldrich and dissolved to a concentration of 5% in 1-2-dichlorobenzene (analytical pure). The polymethyl methacrylate (PMMA) as the dielectric layer was used as purchased from MicroChem, with a molecular weight of 350,000 and a concentration of 4% in anisole (analytical pure).

2.2. Preparation of PDMS/SiO_2 Composite Template by Dry Blending

The experimental procedure for preparing the PDMS/SiO_2 composite template by dry blending is shown in Figure 1.

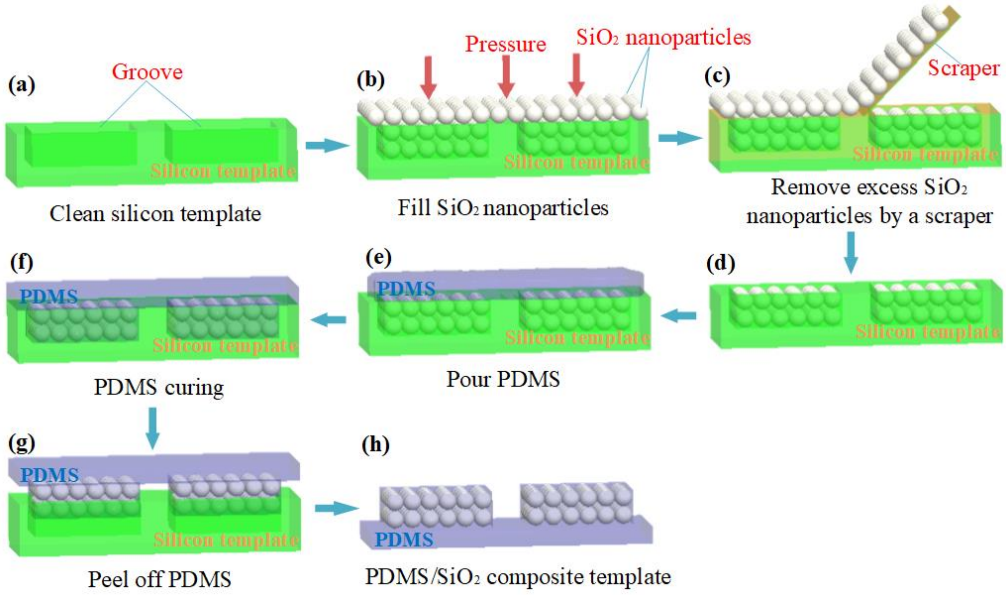

Figure 1. The experimental procedure for preparation of the PDMS/SiO_2 composite template by dry blending: (**a**) clean silicon template; (**b**) fill SiO_2 nanoparticles; (**c**) remove excess SiO_2 nanoparticles; (**d**) fill SiO_2 nanoparticles in the groove; (**e**) pour PDMS; (**f**) PDMS curing; (**g**) peel off PDMS; and (**h**) prepared PDMS/SiO_2 composite template.

First, a silicon template prepared by photolithography with a source-drain structure groove was ultrasonically cleaned for 15 min in an ultrasonic system and dried by nitrogen. Subsequently, the surface of the silicon template was covered with SiO_2 nanoparticles and gently pressed with a glass slide to completely fill the SiO_2

nanoparticles in the groove. The excess SiO_2 nanoparticles outside the groove of the silicon template were then removed by a scraper. PDMS and the curing agent were then thoroughly mixed at a weight ratio of 10:1 and poured it onto the surface of the silicon template. Thereafter, evacuation was performed for 10 min with a vacuum pump, while the PDMS penetrated the SiO_2 nanoparticle gaps and was cured at 30 °C for 24 h. Finally, the PDMS/SiO_2 composite template was prepared by peeling off the PDMS from the silicon template.

2.3. Characterization

The surface morphology of the PDMS/SiO_2 composite template and the OTFT electrodes was investigated by scanning electron microscopy (SEM, JSM-6390a, Japan). The thermal expansion of the PDMS/SiO_2 composite template was examined using a thermomechanical analyzer (TMA, Q400, TA Instruments, New Castle, DE, USA). Five specimens per group with dimensions 20 × 2 × 1 mm were prepared and calculate the strain average. During the test, the temperature was increased from 20 °C to 200 °C at a rate of 20 °C/min. The CTE of the PDMS/SiO_2 composite template was determined based on the curves from the analyzer.

3. Results and discussion

3.1. Surface Morphology of the PDMS/SiO_2 Composite Template

The silicon template prepared and that before and after filling the SiO_2 nanoparticles are shown in Figure 2.

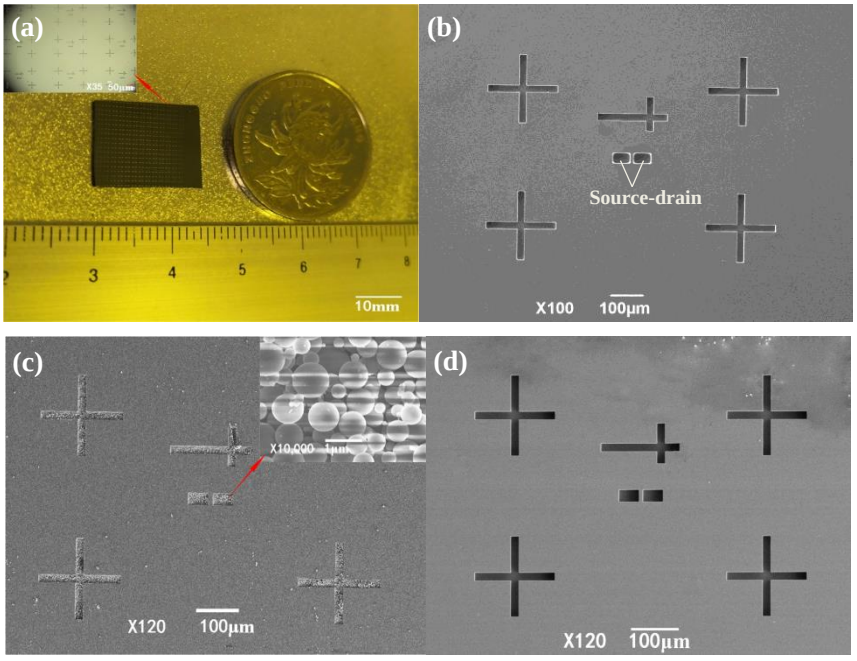

Figure 2. Surface morphology of the silicon template. (**a**) Physical appearance of the silicon template with source-drain groove. (**b**) Groove morphology before filling the SiO_2 nanoparticles. (**c**) Groove morphology after filling the SiO_2 nanoparticles and distribution of nanoparticles in the

groove. (**d**) Groove morphology of the silicon template after peeling off PDMS.

Figure 2a shows the physical appearance of the silicon template etched into the source-drain groove structure. The pattern of the array distribution is presented in the upper left corner of Figure 2a, with the lines uniform and regular. Figure 2b shows the groove morphology before filling the SiO_2 nanoparticles. It is clear from the groove structure of size 50 × 30 μm that the inside is empty, and the surface of the silicon template is clean. Figure 2c shows the groove morphology after filling with SiO_2 nanoparticles. Numerous nanoparticles are in the groove, and there is no surplus of nanoparticles on the surface of the silicon template. The magnified image of the distribution of SiO_2 nanoparticles in the groove at 10,000 multiple is shown in the upper right corner of Figure 2c, which the nanoparticles filled in the groove are uniformly distributed and regularly arranged. Figure 2d shows the groove morphology of the silicon template after peeling off PDMS film. There are no nanoparticles in the groove, demonstrating that PDMS completely draws out the SiO_2 nanoparticles in the groove.

The PDMS/SiO_2 composite template prepared by dry blending is shown in Figure 3.

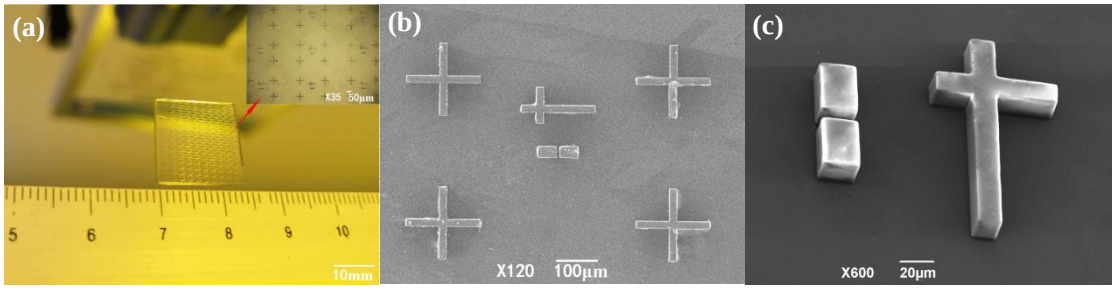

Figure 3. Surface morphology of the PDMS/SiO_2 composite template. (**a**) Physical appearance of the PDMS/SiO_2 composite template. (**b**) Microstructure of the PDMS/SiO_2 composite template. (**c**) Cross-sectional microstructure of the PDMS/SiO_2 composite template.

Figure 3a shows the physical appearance of the PDMS/SiO_2 composite template having a size of 15 × 15 × 1 mm, with the microstructure of the array distribution on the template surface in the upper right corner. Figure 3b shows the microstructure of the PDMS/SiO_2 composite template. The width is uniform and the structure is complete, and the surface of the composite template is clean. The cross-sectional morphology of the composite template is shown in Figure 3c. The edges of columnar microstructure are smooth and complete, which indicates that the PDMS template can be well peeling from the silicon template.

3.2. Calculating the Weight Fraction of the SiO_2 Nanoparticles

To calculate the weight fraction of the SiO_2 nanoparticles filled by dry blending, it is necessary to first calculate the volume fraction of the SiO_2 nanoparticles in the

groove. For the convenience of calculation, we assume that the SiO_2 nanoparticles are filled with uniform distribution and regular arrangement of Figure 1b. SiO_2 nanoparticles with a particle size of 500 nm are filled into a source-drain structure groove with an etching size of 50 × 30 × 25 μm. Hence, the weight fraction of the SiO_2 nanoparticles is calculated according to Equation (1) [20]

$$\omega = \frac{\rho_m \cdot \upsilon}{\rho_m \cdot \upsilon + \rho_n \cdot (1-\upsilon)} \quad (1)$$

.

Here, ω is the weight fraction of the SiO_2 nanoparticles, ρ_m is the density of SiO_2 (2648 kg·m^{-3} [18]), ρ_n is the density of PDMS (965 kg·m^{-3} [20]), and υ is the volume fraction of the SiO_2 nanoparticles (65.4 vol%). The calculated weight fraction of the SiO_2 nanoparticles filled by dry blending is 83.8 wt%, which shows that the SiO_2 nanoparticles have the highest content in the PDMS/SiO_2 composite template.

3.3. CTE of the PDMS/SiO_2 Composite Template

The strain-temperature curves of the PDMS/SiO_2 composite template were investigated with a TMA as shown in Figure 4. For comparison, the PDMS/SiO_2 composite template with nanoparticle content of 0 wt%, 10 wt%, 15 wt%, and 20 wt%, respectively, prepared by wet blending which different contents of SiO_2 nanoparticles were dispersed into PDMS using ultrasonic technology, and their curves are also shown in Figure 4.

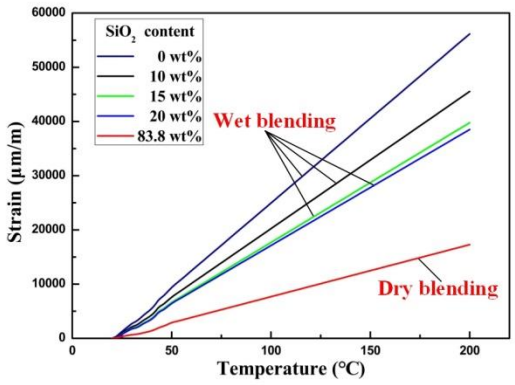

Figure 4. Strain-temperature curves of PDMS/SiO_2 composite templates prepared by dry blending and wet blending

The curves for 0 to 20 wt% of SiO_2 nanoparticles in Figure 4 are the strain-temperature curves for the PDMS/SiO_2 composite template prepared by wet blending, while that for 83.8 wt% of the nanoparticles is the strain-temperature curve for the template prepared by dry blending. The curve for the template prepared by dry blending exhibits the slowest strain rise with increasing temperature, compared to the

curves for the template prepared by wet blending.

Because the temperature increase was not stable in the range of 20 °C to 50 °C, the curves were distorted. To calculate the CTEs of the PDMS/SiO_2 composite templates, the slope of the straight line in the temperature range of 50 °C to 200 °C was used. The relationship between the CTEs of the PDMS/SiO_2 composite templates and the content of the SiO_2 nanoparticles was calculated and is shown in Figure 5.

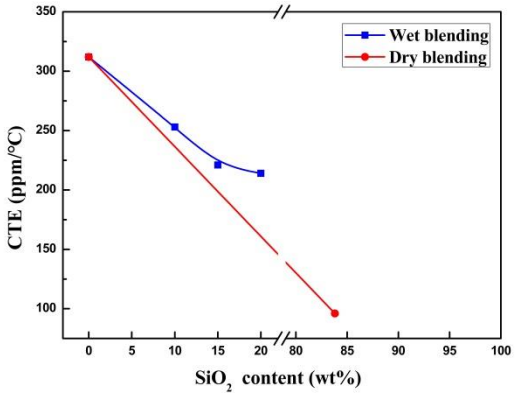

Figure 5. The relationship between the CTEs and content of SiO_2 nanoparticles

Figure 5 shows the relationship between the CTEs of the PDMS/SiO_2 composite templates prepared by wet blending and dry blending and the content of SiO_2 nanoparticles. The curve for the template prepared by wet blending shows that with a gradual increase in the content of SiO_2 nanoparticles to 15 wt%, the CTE of the PDMS/SiO_2 composite template gradually decreases from 312 ppm/°C (original PDMS) to 221 ppm/°C. When the content of the SiO_2 nanoparticles continues to increase to 20 wt%, the CTE of the composite template slowly decreases to 214 ppm/°C. This is primarily because the SiO_2 nanoparticles in PDMS approach saturation, causing the nanoparticles to be dispersed unevenly, due to which, the influence of the nanoparticles on the CTE of PDMS is reduced. However, the curve for the template prepared by dry blending shows that with increasing content of SiO_2 nanoparticles, the CTE of the PDMS/SiO_2 composite template decreases significantly to 96 ppm/°C. Compared with the template prepared by wet blending, the significant decrease in the CTE of the PDMS/SiO_2 composite template prepared by dry blending is mainly attributed to the following two factors. On the one hand, the CTE of SiO_2 is only 0.54 ppm/°C [12]. The higher content of SiO_2 nanoparticles with a low CTE, the greater the influence on the CTE of PDMS. On the other hand, covalent bonds were formed between SiO_2 nanoparticles and PDMS and hydrogen bonds were formed between SiO_2 nanoparticles [14,21]. The higher content of SiO_2 nanoparticles, the greater the interaction among the bonds between PDMS and SiO_2 nanoparticles; this

restricts the thermal deformation of PDMS. Hence, the CTE of the PDMS/SiO_2 composite template significantly decreases.

To verify that the CTE of the PDMS/SiO_2 composite template was reasonable, we compared the CTE with that calculated from a model employing the governing Equation (2) [22]. This equation can be applied to polymer composites filled with one type of nanoparticles.

$$\alpha_c = \alpha_m(1-\phi) + \alpha_p\phi \quad (2)$$

Here, α_c is the CTE model value of the PDMS/SiO_2 composite template, α_m is the CTE of the original PDMS (312 ppm/°C), α_p is the CTE of SiO_2 nanoparticles (0.54 ppm/°C), and ϕ is the volume fraction of the SiO_2 nanoparticles (65.4 vol%). The CTE model value of the composite template was calculated to be 108.3 ppm/°C, which is close to the CTE of the PDMS/SiO_2 composite template prepared by dry blending.

3.4. OTFT Electrodes Alignment

Based on the above analysis, we sputtered approximately 400 nm thick metallic silver as the OTFT electrodes on the surface of the PDMS/SiO_2 composite template prepared by dry blending. We then used the template with silver electrodes for gate and source-drain alignment through a printing process [3,23]. For comparison, the PDMS/SiO_2 composite template (20 wt%) prepared by the wet blending was subjected to the same experiment, as shown in Figure 6.

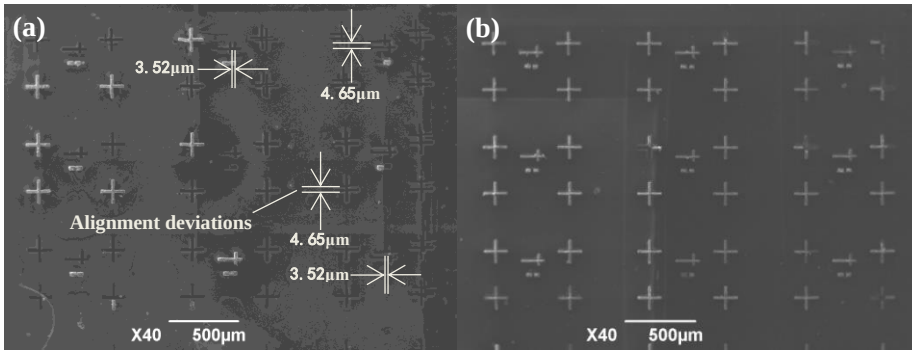

Figure 6. OTFT electrodes alignment. (**a**) Electrode alignment of the 20 wt% composite template prepared by wet blending. (**b**) Electrode alignment of the 83.8 wt% composite template prepared by dry blending.

Figure 6a shows the electrode alignment of the PDMS/SiO_2 composite template (20 wt%) prepared by wet blending. The alignment of the gate and source-drain is deviated during the experiment, which shows that the vertical deviations are about 4.65 μm and the horizontal deviations are about 3.52 μm. The difference is that the composite template (83.8 wt%) prepared by dry blending achieves well alignment of

the gate and source-drain (Figure 6a). The reason for deviations of the electrode alignment in the wet-blended template is that the CTE of the PDMS/SiO_2 composite template is 214 ppm/°C, while that of the PMMA dielectric layer to be contacted is 115.2 ppm/°C [24]. The CTE of the PDMS/SiO_2 composite template prepared by dry blending was 96 ppm/°C, which better matches that of the dielectric layer.

4. Conclusions

In this study, we propose a novel dry blending method in which SiO_2 nanoparticles are filled into a grooved silicon template, following which PDMS permeates the SiO_2 nanoparticle gaps. The SiO_2 nanoparticles in the groove are brought out by curing and peeling off the PDMS to prepare the PDMS/SiO_2 composite template. The results show that the content of SiO_2 nanoparticles in the PDMS/SiO_2 composite template is 83.8 wt%. Moreover, the CTE of the composite template is 96 ppm/°C, and is reduced by 69.23% compared to that of the original PDMS template. Using the dry-blended composite template with the low CTE, alignment between the gate and the source-drain during the printing process is achieved, which is of great significance in improving the performance of the OTFT.

References

[1] Myny K. The development of flexible integrated circuits based on thin-film transistors [J]. Nature Electronics, 2018, 1(1): 30-39.

[2] Shi Y, Guo H, Qin M, et al. Thiazole Imide- Based All- Acceptor Homopolymer: Achieving High- Performance Unipolar Electron Transport in Organic Thin- Film Transistors [J]. Advanced Materials, 2018, 30(10): 1705745.

[3] Song D, Secor E B, Wang Y, et al. Transfer Printing of Sub-5 μm Graphene Electrodes for Flexible Microsupercapacitors [J]. ACS applied materials & interfaces, 2018, 10(26): 22303-22310.

[4] Kim S M, Kim C H, Kim Y, et al. Influence of PEDOT: PSS crystallinity and composition on electrochemical transistor performance and long-term stability [J]. Nature communications, 2018, 9(1): 3858.

[5] Wang N, Yang A, Fu Y, et al. Functionalized Organic Thin Film Transistors for Biosensing [J]. Accounts of chemical research, 2019, 52(2): 277-287.

[6] Yang L, Gu B, Chen Z, et al. Synthetic Biopigment Supercapacitors [J]. ACS applied materials & interfaces, 2019, 11(33): 30360-30367.

[7] Ibanez J G, Rincón M E, Gutierrez-Granados S, et al. Conducting polymers in the fields of energy, environmental remediation, and chemical–chiral sensors [J]. Chemical reviews, 2018, 118(9): 4731-4816.

[8] Malik A, Kandasubramanian B. Flexible Polymeric Substrates for Electronic Applications [J]. Polymer Reviews, 2018, 58(4): 630-667.

[9] Gensch M, Schwartzkopf M, Ohm W, et al. Correlating Nanostructure, Optical and Electronic Properties of Nanogranular Silver Layers during Polymer-Template-Assisted Sputter Deposition [J]. ACS applied materials & interfaces, 2019, 11(32): 29416-29426.

[10] Shokrieh M M, Daneshvar A. A Novel Technique to Simulate Reduced Residual Stresses in Laminated Composites Using Nanoparticles [J]. Iranian Journal of Science and Technology, Transactions of Mechanical Engineering, 2019, 43(1): 17-26.

[11] González-Benito J, Castillo E, Caldito J F. Coefficient of thermal expansion of TiO_2 filled EVA based nanocomposites. A new insight about the influence of filler particle size in composites [J]. European Polymer Journal, 2013, 49(7): 1747-1752.

[12] Ren L, Pashayi K, Fard H R, et al. Engineering the coefficient of thermal expansion and thermal conductivity of polymers filled with high aspect ratio silica nanofibers [J]. Composites Part B: Engineering, 2014, 58: 228-234.

[13] Jeyranpour F, Alahyarizadeh G, Minuchehr A. The thermo-mechanical properties estimation of fullerene-reinforced resin epoxy composites by molecular dynamics simulation–A comparative study [J]. Polymer, 2016, 88: 9-18.

[14] Liu J, Zong G, He L, et al. Effects of fumed and mesoporous silica nanoparticles on the properties of sylgard 184 polydimethylsiloxane [J]. Micromachines, 2015, 6(7): 855-864.

[15] Kalsoom U, Peristyy A, Nesterenko P N, et al. A 3D printable diamond polymer composite: a novel material for fabrication of low cost thermally conducting devices [J]. RSC Advances, 2016, 6(44): 38140-38147.

[16] Wang Y W, Chen W C. Synthesis, properties, and anti-reflective applications of new colorless polyimide-inorganic hybrid optical materials [J]. Composites Science and Technology, 2010, 70(5):769-775.

[17] Nugroho F A A, Darmadi I, Cusinato L, et al. Metal–polymer hybrid nanomaterials for plasmonic ultrafast hydrogen detection [J]. Nature materials, 2019, 18(5): 489.

[18] Saraswathi M S S A, Nagendran A, Rana D. Tailored polymer nanocomposite membranes based on carbon, metal oxide and silicon nanomaterials: a review [J]. Journal of Materials Chemistry A, 2019, 7(15): 8723-8745.

[19] Wang H, Hor J L, Zhang Y, et al. Dramatic Increase in Polymer Glass Transition Temperature under Extreme Nanoconfinement in Weakly Interacting Nanoparticle Films [J]. ACS nano, 2018, 12(6): 5580-5587.

[20] Li H, Tao Y, Zhang C, et al. Dense graphene monolith for high volumetric energy density Li–S batteries [J]. Advanced Energy Materials, 2018, 8(18): 1703438.

[21] Suzuki N, Kamachi Y, Takai K, et al. Effective use of mesoporous silica filler: comparative study on thermal stability and transparency of silicone rubbers loaded with various kinds of silica particles [J]. European Journal of Inorganic Chemistry, 2014, 2014(17): 2773-2778.

[22] Kurimoto M, Ozaki H, Sawada T, et al. Filling ratio control of TiO_2 and SiO_2 in epoxy composites for permittivity-graded insulator with low coefficient of thermal expansion [J]. IEEE Transactions on Dielectrics and Electrical Insulation, 2018, 25(3): 1112-1120.

[23] Kim J, Chae D, Lee W H, et al. Enhanced performance and reliability of organic thin film transistors through structural scaling in gravure printing process [J]. Organic Electronics, 2018, 59: 84-91.

[24] Thomas P, Dakshayini B S, Kushwaha H S, et al. Effect of Sr_2TiMnO_6 fillers on mechanical, dielectric and thermal behaviour of PMMA polymer [J]. Journal of Advanced Dielectrics, 2015, 5(03): 1550018.